Journal of Hydrology 578 (2019) 124052

Contents lists available at ScienceDirect

Journal of Hydrology

journal homepage: www.elsevier.com/locate/jhydrol

Research papers

Estimation of lake water storage and changes based on bathymetric data and altimetry data and the association with climate change in the central Tibetan Plateau

Baojin Qiao[a,b,*], Liping Zhu[b,c,d,*], Junbo Wang[b,c], Jianting Ju[b], Qingfeng Ma[b], Lei Huang[b,d], Hao Chen[b,d], Chong Liu[b,d], Teng Xu[b,d]

[a] Institute of Smart City, Zhengzhou University, Zhengzhou 450001, China
[b] Key Laboratory of Tibetan Environment Changes and Land Surface Processes, Institute of Tibetan Plateau Research, Chinese Academy of Sciences (CAS), Beijing 100101, China
[c] CAS Center for Excellence in Tibetan Plateau Earth Sciences, Beijing 100101, China
[d] University of Chinese Academy of Sciences, Beijing 100049, China

ARTICLE INFO

This manuscript was handled by Marco Borga, Editor-in-Chief

Keywords:
Bathymetric data
Water storage
Lake expansion
Glacial meltwater

ABSTRACT

Lake water storage is an important factor in analyses of lake water balance. However, it is difficult to calculate the water storage of lakes on the Tibetan Plateau due to the lack of bathymetric data. Lake water storage and changes in Chibuzhang Co (CC) and Duoersuodong Co (DC), which are located in an endorheic system and have been connected since 2006, were estimated based on in situ bathymetric data, satellite altimetry data and Landsat images of the central Tibetan Plateau. In 2016, the maximum depth and water storage of DC were 68.7 m and 12.2 ± 1.72 km^3, respectively, with an area of 490.2 km^2, and those of CC were 116.3 m and 16.2 ± 2.27 km^3, respectively, with an area of 575.4 km^2. The total lake water storage in DC and CC increased by 24.5% (2.4 km^3) and 14.1% (2 km^3) from 2003 to 2014, respectively, based on satellite altimetry data and Landsat images using an empirical equation. The relationship between lake changes and meteorological factors indicated that both increased glacial meltwater and increased precipitation were important drivers of each lake's expansion and that a small increase in evaporation (2.5 mm/y) had little negative impact on lake expansion (0.41 m/y). Heterogeneous changes in the two lakes from 1993 to 2005 were mainly due to water from CC supplying DC through a channel, and the lake level of DC was always lower than that of CC until 2006, indicating that the geological conditions around both lakes were also an important factor in the lake changes. The assumption was that all glacial meltwater from the Puruogangri and Geladandong glaciers was supplied to the two lakes through runoff with minimal evaporation, and glacial meltwater made an approximately 19.3 ± 4.5% contribution to the lake expansions (0.4 km^3/y) of DC and CC from 2003 to 2014 based on the results of the glacier mass balance.

1. Introduction

The Tibetan Plateau (TP) has been described as the "Third Pole" and the "Asian water tower", and many of the major Asian rivers that originate on the TP are maintained by surface runoff (Immerzeel et al., 2010), e.g., the Yellow River, Yangtze River, and Brahmaputra River, which together supply water to nourish hundreds of millions of people. There many glaciers and lakes across the TP, which are sensitive to climate change and have considerable influence on the regional hydrological cycle through land breeze circulation and changes in regional precipitation (Samuelsson and Tjernström, 2001; Zhao et al., 2012). The climate of the TP has experienced great changes in recent decades, and the air temperature (0.036 °C/y) and lake surface temperature (0.03 °C/y) showed rising trends from 2001 to 2012 according to the Moderate-resolution Imaging Spectroradiometer (MODIS) land surface temperature data (Zhang et al. 2014b). Nearly 90% of the meteorological stations on the TP showed increased annual precipitation from 1961 to 2001 (Xu et al. 2008). Most glaciers on the TP have experienced significant shrinkage, but most lakes on the TP have experienced a rapid expansion since 1994, except for several lakes in the

* Corresponding authors at: Institute of Smart City, Zhengzhou University, Zhengzhou 450001, China (B. Qiao). Key Laboratory of Tibetan Environment Changes and Land Surface Processes, Institute of Tibetan Plateau Research, Chinese Academy of Sciences (CAS), Beijing 100101, China (L. Zhu).
E-mail addresses: qiaobaojin@zzu.edu.cn (B. Qiao), lpzhu@itpcas.ac.cn (L. Zhu).

https://doi.org/10.1016/j.jhydrol.2019.124052
Received 25 April 2019; Received in revised form 15 August 2019; Accepted 17 August 2019
Available online 19 August 2019
0022-1694/

southern TP since 2000 (Lei et al., 2014; Li et al., 2014b; Phan et al., 2012; Wang et al., 2013; Song et al., 2013, 2014a,b; Yao et al., 2012; Zhang et al., 2011b, 2014a, 2017). Lake expansion floods roads and meadows; therefore, lake expansion has a serious influence on the regional environment and animal husbandry, and many studies have analyzed the causes of lake changes.

Most previous studies have mainly focused on lake areas (Wan et al., 2014; Zhang et al., 2014a, 2015) and lake levels (Phan et al., 2012; Song et al., 2014a; Zhang et al., 2011b), whereas only a few studies have focused on changes in lake water storage (Qiao et al., 2019; Qiao and Zhu, 2017; Song et al., 2014a; Zhang et al., 2011b, 2017). Lake water storage change is a better indicator of responses to climate change than lake area change because the topographic conditions around lakes are different (Qiao et al., 2017). For example, a lake with steep slopes may experience less area change than a lake in a gently sloping basin, even though the former may receive more inflowing water than the latter. Lake water storage change can be estimated by combining satellite radar altimetry data and Landsat images. The Ice, Cloud and Land Elevation Satellite (ICESat), with a 70 m footprint, has been widely used to study lake level and water storage changes in large lakes (Li et al., 2014b; Phan et al., 2012; Song et al., 2013; Wang et al., 2013; Zhang et al., 2011b) from 2003 to 2009. The CryoSat-2 mission was launched in April 2010; the altimetry data from the satellite provided Earth surface measurements with a footprint of approximately 290 m, which were also used to analyze lake levels and water storage changes in large lakes with high precision (Jiang et al., 2017; Kleinherenbrink et al., 2015; Lee et al., 2016; Song et al., 2015a,b).

Lake water storage and underwater topography are also important information in lake research. The variation in lake heat storage is an important component used for estimating evaporation in deep lakes, where the lake heat storage is dependent upon absolute water storage (McMahon et al., 2013). The underwater topography of large lakes is very helpful for further studies of the paleoenvironment and water energy conversions, e.g., how to select a suitable site for sediment drilling (Wang et al., 2017; Xu et al., 2019) and water temperature observations at different depths (Huang et al., 2017; Lazhu et al., 2015). There is little research on lake water storage and underwater topography due to the lack of bathymetric data and other available data. If the bathymetric data of the lake are known, the underwater topography and water storage can be calculated using a spatial interpolation method. However, most lakes on the TP are distributed across remote regions that are inaccessible, and only a few lakes have been surveyed using bathymetric equipment, e.g., Nam Co (Zhang et al., 2011a), four lakes on the northwestern TP (Qiao et al., 2017), and Paiku Co on the southern TP (Lei et al., 2018).

The cause of TP lake changes is still debated, and some previous studies considered that increased precipitation may be the main cause of lake expansion based on an analysis of the relationship between the annual precipitation change trend and annual lake area and lake level changes and by quantifying the contribution of each factor to lake change using a hydrological model (Lei et al., 2013; Song et al., 2014b; Zhou et al., 2015). By analyzing the annual change in lake surface evaporation, researchers found that decreasing lake evaporation contributed approximately 4% to the rapid lake expansion of Nam Co (Ma et al., 2016). Li et al. (2014b) speculated that the main cause of TP lake expansion was permafrost degradation because most lake expansion had occurred in the area of the TP where considerable permafrost was distributed and glaciers experienced less retreats.

However, based on the measurement data and remote sensing images, most glaciers have experienced significant shrinkage on the TP (Yao et al., 2012). Increased glacial meltwater may have an important contribution to lake expansion (Li et al., 2014a; Meng et al., 2011; Zhang et al., 2011b, 2015; Zhu et al., 2010). According to a comparison of the glacier elevation differences in the five pairs of TanDEM CoSSC datasets between 2013 and 2014 and SRTM in 2000, the decadal glacier mass balance in the Western Nyainqentanglha Mountains was calculated for the 2000 to 2014 period, and the results indicated that the contribution of glacial meltwater to the lake expansion of Nam Co was likely 10.5 ± 9% (Li and Lin, 2017). A comparison of the glacier surface elevation difference between SPOT-6/7 stereo imagery and SRTM revealed that glacial meltwater contributed 9.9% and 11.1% to the lake expansions of LexieWudan Lake and KekeXili Lake, respectively, on the central TP (Zhou et al., 2019). The results of Zhu et al. (2010) indicated that although precipitation played a dominant role in maintaining the water balance, increased glacial meltwater made a 50.6% contribution to the lake expansion of Nam Co based on a quantification of the proportions of different factors. Glacial meltwater was considered to have made an equivalent contribution to lake expansion with precipitation-evaporation according to a comparison of the difference between the change in water storage of glacier-fed and non-glacier-fed lakes in the Tanggula Mountains (Song and Sheng, 2016), northwestern TP (Qiao and Zhu, 2017) and inner TP (Qiao and Zhu, 2019). Due to the lack of reliable measurement data on mass balance and meteorological data, quantification of the contribution of glacial meltwater to lake expansion has mainly concentrated on several large lakes, and many more lakes must be included in future studies.

In this paper, the lake depth distributions of CC and DC, which are located in an endorheic system on the central TP, were surveyed in 2016 using a Lowrance HDS5 instrument. The bathymetric data were used to establish the underwater topography and estimate lake water storage. We estimated lake water storage changes over a long time scale from 2003 to 2014 by combining altimetry data (ICESat and CryoSat-2) and Landsat images. The purposes of this study were as follows: (1) to analyze the characteristics of the underwater topography and estimate water storage; (2) to estimate changes in water storage from 2003 to 2014; (3) to analyze the possible linkage between lake changes and climatic factors; and (4) to quantify the contribution of glacial meltwater to lake expansion.

2. Study area

The study region is located in the transitional zone between the monsoon-dominated south and the dry, continental westerly-dominated north (Thompson et al., 2006). The annual average temperature of this region is approximately −4 °C based on data from the regional meteorological station, and the annual precipitation is less than 500 mm, with 90% of the precipitation occurring from May to September (Zhou et al., 2014). Puruogangri is one of the largest ice fields outside of the Arctic and Antarctic, with a glacier area of approximately 420 km^2 and an ice volume of approximately 52 km^3 (Yi et al., 2002). The ice core records from the Puruogangri glaciers suggested that abrupt warming began in the early 20th century and continued until 2000, and this region was influenced more by continental climatic processes than by the monsoon because the low/high $\delta^{18}O$ was similar to that in the Dunde ice core to the north, but opposite to that in the Dasuopu ice core in the Himalayas (Thompson et al., 2006). Strengthened westerlies would increase the precipitation in this region (Yao et al., 2012). Understanding the changes in lake levels and water storage in lakes fed by this ice cap would help to complement information provided by the paleoclimate records.

Most TP lakes are tectonic lakes, and the total watershed of the study region is located in a large discontinuous mountain basin controlled by the Bangong-Nujiang tectonic belt. As shown in Fig. 1, CC (90.37°E, 33.47°N) and DC (89.90°E, 33.43°N) are twin lakes that are connected by a channel. In the initial period (pre-2006), only DC was endorheic, while water from CC flowed into DC through a channel; during the later period, both lakes merged and formed one single endorheic system (Jiang et al., 2017). The levels of the two lakes increased quickly over the last decade and increased glacial meltwater may have made similar contribution to lake expansion as that of precipitation-evaporation (Song and Sheng, 2016). CC receives a glacial meltwater supply from the Geladandong glaciers via three large rivers,

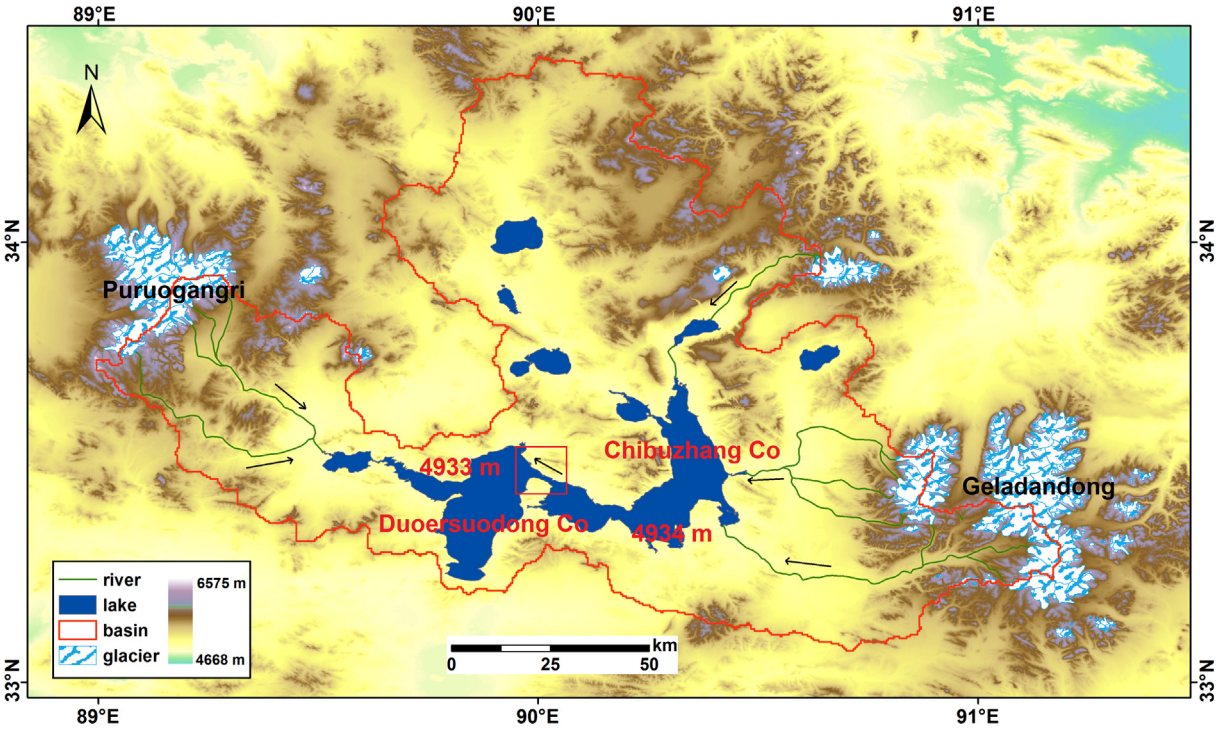

Fig. 1. Location and topography of the study region. The red polygon represents the location of the water channel; 4933 m and 4944 m represent the lake levels of each lake in 2005, and the arrow represents the direction of water flow. (For interpretation of the references to color in this figure legend, the reader is referred to the web version of this article.)

Table 1
the detailed information of Landsat images used in this study.

Year	Data Label	Time	Cloud (%)
1976	LM21490371976317AAA02	1976–11–12	90
1988	LT51390371988288BKT00	1988–10–14	1.7
1990	LT51390371990309BJC00	1990–11–5	26.23
1992	LT51390371992315ISP00	1992–11–10	11.46
1993	LT51390371993301ISP00	1993–10–28	14.38
1996	LT51390371996294ISP00	1996–10–20	17.15
1998	LT51390371998251BIK00	1998–9–8	27.79
2000	LE71390372000281SGS00	2000–10–7	1.03
2001	LE71390372001267SGS01	2001–9–24	1.05
2002	LE71390372002238SGS00	2002–8–26	1.35
2003	LT51390372003281BJC00	2003–10–8	10.28
2004	LT51390372004284BJC00	2004–10–10	10.73
2005	LT51390372005318BKT00	2005–11–14	15
2006	LT51390372006257IKR00	2006–9–14	20
2007	LT51390372007260IKR00	2007–9–17	0
2008	LT51390372008279BKT00	2008–10–5	2.46
2009	LT51390372009313BKT00	2009–11–9	22.77
2010	LE71390372010292SGS00	2010–10–19	29.57
2011	LE71390372011327PFS00	2011–11–23	3.39
2012	LE71390372012314PFS00	2012–11–9	3.3
2013	LC81390372013340LGN01	2013–12–6	3.68
2014	LC81390372014279LGN00	2014–10–6	9.3
2015	LC81390372015250LGN00	2015–9–7	6.33
2016	LC81390372016317LGN00	2016–11–12	2.03

which are located on the eastern side of this lake, approximately 60 km from CC (Fig. 1). An upstream lake is located in the northeastern part of CC. DC also receives a glacial meltwater supply from the Puruogangri glaciers through a large river (Fig. 1), which is located to the west of this lake, approximately 50 km from DC. Glacier surface elevation changes have been reported based on different methods; specially, the glacier surface elevation decreased by 6.2 m from 1974 to 2000 (Lei et al., 2012) and by -0.046 ± 0.082 m w.e.a^{-1} from 2000 to 2011 (Zhang et al., 2018), and the thinning rate was -0.317 ± 0.027 m/y from 2012 to 2016 (Liu et al., 2016). Most glaciers in the Tangguala Mountains have been retreating since the 1960s (Tseng et al., 2016). The Geladandong glacier area decreased by 66.68 km^2 (7.37% of the total glacier area) from 1992 to 2009 (Zhou et al., 2014), and the glacier surface elevation thinning rate was -0.22 ± 0.12 m/y from 1973 to 2000 (Zhou et al., 2018) based on ICESat laser altimetry measurements and -0.243 ± 0.066 m w.e.a^{-1} from 2000–2016 (Zhang et al., 2018) based on MODIS albedo products.

3. Methods

3.1. Multi-temporal Landsat images for lake area extraction

Landsat Multispectral Scanner/Thematic Mapper (TM)/Enhanced Thematic Mapper Plus (ETM+)/Operational Land Image images were used to extract the lake areas. Because no images were available for the years 1989, 1991, 1995, 1997 and 1999, we only calculated the lake area in 1976, 1988, 1990, 1992, 1993, 1994, 1996, and 1998 and from 2000 to 2016. These images were downloaded from the U.S. Geological Survey (http://glovis.usgs.gov/). The lake level of most lakes on the TP showed large increases during the warm seasons (March–October) and declines or minor fluctuations during the cold seasons (November–February) (Song et al. 2014a). To compare the inter-annual changes and reduce the seasonal variation influence, only the images obtained between September and November were selected because the lake levels were at their highest during these months, allowing us to compare the largest area change of the lakes over a given year in recent decades. The highest quality images with the least amount of clouds and snow were prioritized, and detailed information on the images use is provided in Table 1. The Normalized Difference Water Index (NDWI) method was used to extract the lake areas (McFeeters, 1996).

The detailed process of this method is as follows: (1) the image was processed by radiometric correction to eliminate or correct image distortion caused by radiation error process; (2) the band ratio method was used with the green band and near infrared (NIR) band to calculate the

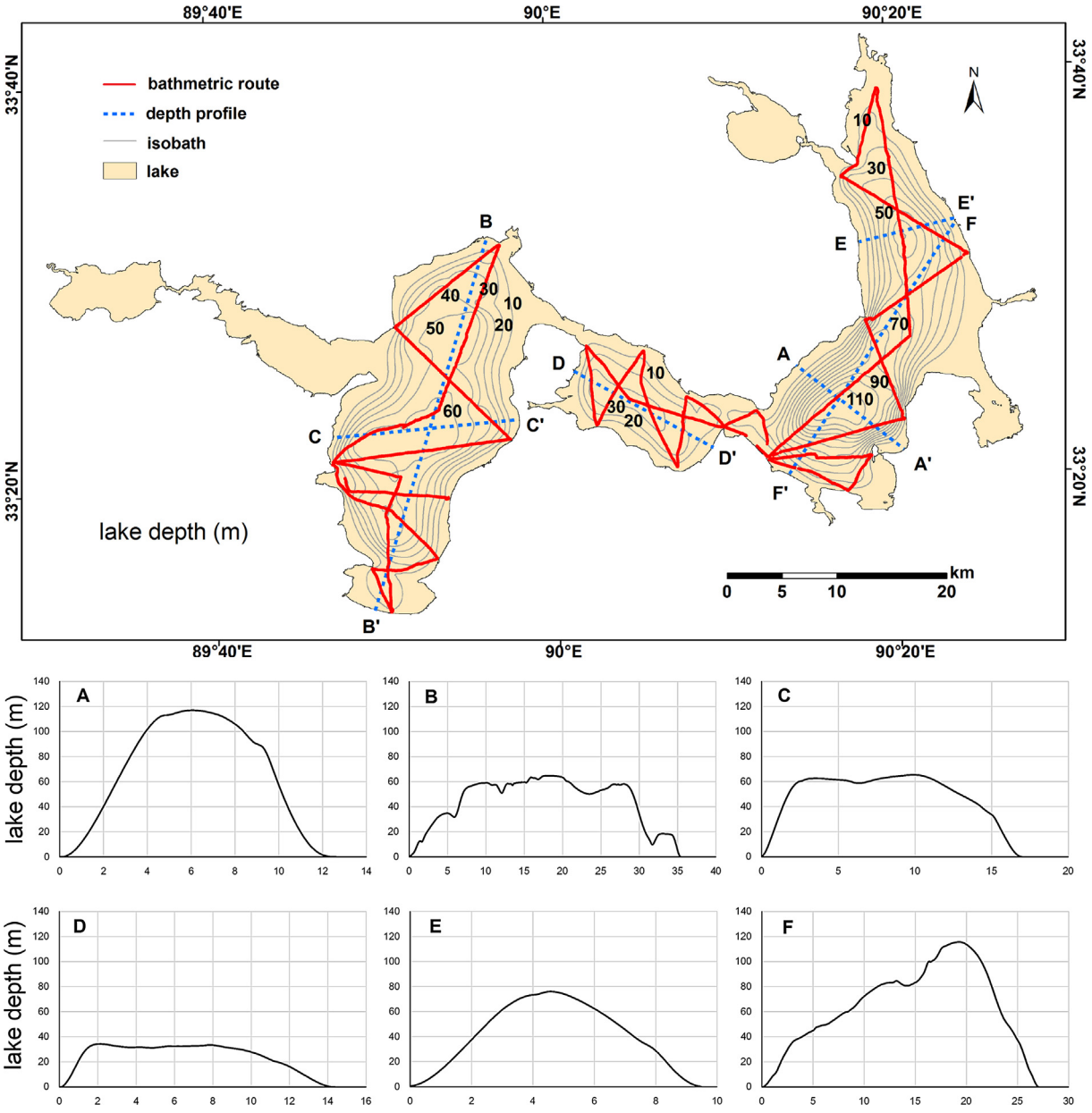

Fig. 2. Depth isobaths (thin gray line) and profile route (blue line) based on the bathymetric data. A and A' represent the starting point and ending point of the profile, respectively. The red line represents the bathymetric route. (For interpretation of the references to color in this figure legend, the reader is referred to the web version of this article.)

pixel value ratio in different bands of the same image, with the equation NDWI = (Green − NIR)/(Green + NIR); (3) the color slice range of 0–1 was chosen to extract the water body boundary as a shapefile; and (4) the error boundary was modified by manual interpretation.

3.2. Bathymetric data for estimating water storage

Bathymetric data from the lake were surveyed in situ in October 2016. A Lowrance HDS5, which has a vertical accuracy of 0.01 m, was used to survey the lake depth, and bathymetric data were recorded every second. The measured route is shown in Fig. 2; a total of 0.68 million points were measured which covered the main region of the two lakes, except for three small areas, which were located in the western parts of CC and DC and the southeastern part of CC (Fig. 2). All bathymetric data with latitude, longitude and depth used for establishing the underwater topography of two lakes are provided in Appendix. These data were used to estimate lake water storage, which essentially represented the actual lake water storage. We combined the bathymetric data and lake shoreline data to establish the underwater topography, and we assigned the depth value of the lake shoreline as 0 to reduce interpolation bias. The Topo to Raster tool is an interpolation method specifically designed for the creation of a hydrologically correct digital elevation model (DEM), and an iterative finite difference interpolation technique was used (Hutchinson, 1988; 1989). Using spatial analyst tools (Topo to Raster) in ArcGIS 9.3 to establish the underwater topography with grid units of 56 m × 56 m, water storage was estimated based on a given lake depth using the "Area and Volume" tool of 3D Analyst in ArcGIS.

3.3. Altimetry data to calculate lake level change

The altimetry data from ICESat and CryoSat-2 have been widely used to monitor lake level changes on the TP (Jiang et al., 2017; Phan et al., 2012; Song et al., 2014a; Zhang et al., 2011b). The Geoscience

Laser Altimeter System (GLAS) onboard ICESat has provided global altimetry data for approximately 20 one-month campaigns since January 2003 (Song et al., 2013). The National Snow and Ice Data Center (NSIDC) archived all the original datasets and distributed ICESat's Level 2 global land surface altimetry data product (GLA14). We used the NSIDC GLAS Altimetry elevation extractor Tool (NGAT) to extract the time-series elevation with latitude, longitude and geoid information from the GLAS14 altimetry products.

The Narrow Primary Peak Threshold (NPPT) retracker (Jain et al., 2015) was applied to the CryoSat-2 data, which had previously been proven to provide valid results for inland water application (Nielsen et al., 2015; Villadsen et al., 2016).

$$R = R_{wd} + R_r + R_{gc} \quad (1)$$

where R_{wd} is the window delay, R_r is the retracker correction and R_{gc} are the geophysical corrections, including the ionosphere, wet and dry troposphere, solid earth tide, ocean loading tide, and pole tide.

The surface elevation H with respect to the Earth Gravitational Model of 2008 geoid (EGM2008) was obtained using the following equation:

$$H = h - R - N \quad (2)$$

where h is the satellite altitude and N is the geoid height with respect to the ellipsoid.

ICESat and data CryoSat-2 covered the periods from 2003 to 2009 and 2010 to 2015, respectively, and the height of the ICESat data was converted from EGM1996 to EGM2008, which was consistent with the CryoSat-2 data. We calculated the average lake level on the same day as the lake level, and we calculated the standard deviation of these data on the same day to determine the accuracy and bias of the average lake level. We used these data to reconstruct lake level changes from 2003 to 2014.

3.4. Estimation of lake water storage change

There are several methods used to estimate lake water storage change, such as using an empirical equation based on the relationship between lake area and lake level (Qiao et al., 2017; Song et al., 2013; Yang et al., 2017; Zhang et al., 2013) or to estimate based on underwater topography (Qiao et al., 2017; Zhang et al., 2011a). Because three small areas of the two lakes were not measured using bathymetric data, and the lake area change in these two lakes was mainly concentrated in these areas (western DC and southeastern CC), the lake water storage change could not be accurately estimated based on the underwater topography and time-series change in the lake area, as reported by Qiao et al. (2017) and Zhang et al. (2011a). In this study, we obtained the lake level change from the ICESat and CryoSat-2 altimetry data, and the lake area change from multi-temporal Landsat images. An empirical equation was used to estimate water storage changes based on changes in lake area and level;

$$\Delta V = \frac{1}{3} \times (S_1 + \sqrt{S_1 \times S_2} + S_2) \times \Delta h \quad (3)$$

S_1 and S_2 represent the lake areas for two periods, $\triangle h$ represents the lake level change during the two periods, and $\triangle V$ represents the water storage change during the two periods.

3.5. The meteorological data used to analyze the causes of lake variations

The China Meteorological Forcing Dataset (CMFD), covering 1979–2013, was developed by the Institute of Tibetan Plateau Research, Chinese Academy of Sciences (He and Yang, 2011). These datasets were assimilated by combining the meteorological data from 740 stations of the China Meteorological Administration (CMA), Princeton meteorological forcing data (Sheffield et al., 2006) and the Tropical Rainfall Measuring Mission (TRMM) 3B42 precipitation products (Huffman et al., 2007). These datasets included near-surface temperature, precipitation, pressure, wind speed and specific humidity with temporal and spatial resolutions of 3 h and 0.1°, respectively. The dataset was used to analyze the annual precipitation and annual average temperature change trend from 1979 to 2013.

The Penman equation (Penman, 1948) has been widely and successfully used for estimating open water evaporation (McMahon et al., 2013). Because actual evaporation information is difficult to acquire on the TP, we used the Penman equation to estimate the potential evaporation (Ep) of the lake surface water based on data from 56 meteorological stations on the TP and to estimate their spatial distributions using the Kriging interpolation method in ArcGIS. The daily maximum and minimum temperatures, relative humidity, sunshine duration and wind velocity data at each meteorological station were used to calculate Ep from 1976 to 2013:

$$Ep = \frac{\Delta}{\Delta + \gamma}\frac{Rn}{\lambda} + \frac{\gamma}{\Delta + \gamma}\frac{6430(1 + 0.536u2)D}{\lambda} \quad (4)$$

where Rn is the daily net radiation (MJ m^{-2} day^{-1}), $\triangle$ is the slope of the saturation vapor pressure curve (kPa/°C), γ is the psychrometric constant (kPa/°C), D is the vapor pressure deficit (Pa), u_2 is the daily average wind speed at a 2 m height (m/s), and λ is the latent heat of water vaporization (2.45×10^6 J/Kg).

Hoh Xil Lake was near the study region, and the complete ice cover of Hoh Xil lake occurred in the middle of October to early December, and complete melting occurred from early May to the middle of June (Yao et al., 2015). Sublimation from the lake surface ice could be considered negligible due to the low temperature in this region during winter (Ma et al., 2016). We assume that the evaporation from December to April is 0 and that evaporation during the other months represents the annual Ep.

4. Results

4.1. The characteristics of the underwater topography and lake water storage

As shown in Fig. 2, 22 transects were measured, which covered the main region of the two lakes. There were 445,549 and 240,472 measurement points in CC and DC, respectively, and the maximum depths and lake area were 116.3 m and 575.4 km^2, and 68.7 m and 490.2 km^2, respectively. Lake underwater topography and depth isobaths were reconstructed based on the bathymetric data. The maximum depth of CC was located in the southern area of the lake, and the topography was very steep. The maximum depth of DC was located in the central part of the lake; a large area of this region was greater than 60 m deep, and the topography was gentle.

The Profile Graph tools on the 3D Analyst interactive toolbar were used to derive a graphic representation in one profile. Using this tool, six profiles of the two lakes were derived. As shown in Fig. 2, six profiles were derived based on the underwater topography. The maximum depth profiles were profiles A and F, which were located in CC, and the shallowest was profile D, which was located in the western CC. As shown in profiles A, E and F, the underwater topography of CC was very steep, especially in the southern part of this lake, which showed intensive isobaths. The topography of DC was undulating based on profiles B and C, and the average depth was shallower than that of CC. A small lake connects the two large lakes, which is located in the middle of DC and CC, the topography is gentle in this lake, and the maximum depth of this lake is less than 40 m.

Lake water storage can be estimated based on the underwater topography. Because the scope of the bathymetric data did not cover both lakes entirely, with data missing for the western part of DC and the southeastern and northwestern parts of CC, the estimated lake water storage should be less than that of the actual water storage. However, the bathymetric data covered the main region of the two lakes, and we

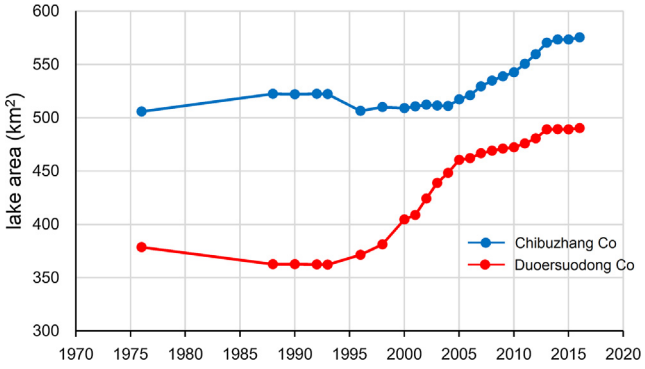

Fig. 3. Lake area change of the two lakes from 1976 to 2016.

are confident that the estimation of lake water storage satisfactorily represents the actual water storage. Based on the underwater topography, the lake water storage of DC was at least 12.2 ± 1.72 km^3, and the average depth of this lake was 31.7 m in 2016. We calculated the lake water storage in CC, including that of the small lake connecting the two large lakes. The water storage of the small lake was at least 1.85 ± 0.26 km^3, and the average depth of this lake was 14.2 m in 2016. The water storage of the main lake in CC was at least 14.3 ± 2.01 km^3, and the average depth of this lake was 37.7 m in 2016. Although the maximum depth of CC was approximately twice that of DC, the average depths of the two lakes were nearly the same.

4.2. Changes in lake area and level

As shown in Fig. 3, the lake area of CC increased slightly from 1976 to 1988, whereas that of DC experienced a decreasing trend during this period. Both lakes remained stable during 1988–1993. CC shrank during 1993–1996 and then remained stable during 1996–2004, and the lake area began to increase after 2005 (5.3 km^2/y). The lake area of DC underwent a rapid increase from 1996 to 2005; subsequently, the increased rate of the lake area (9.9 km^2/y) from 2006 to 2016 was lower than the rate during 1996–2005 (2.8 km^2/y). The two lakes showed different types of changes in the different periods, but both lakes exhibited a rapidly increased rate after 2005.

As shown in Fig. 4a, the standard deviation of the CC lake level was much higher than that of DC, but the lake level of CC was consistent with that of DC after 2010. The lake levels of CC and DC were not consistent before 2006, and the lake level of CC was approximately 1 m higher than that of DC in 2004. According to the SRTM DEM, which acquired DEM data for over 80% of the globe during an 11-day mission in February 2000, the lake level of CC was approximately 6 m higher than that of DC. These results indicated that even though the two lakes were connected by a channel, the amount of water inflow to DC from CC was limited because the channel was narrow before 2006. The increased rate of the DC lake area was much faster during 1996–2005 than that during 2006–2016, but CC exhibited a stable state during 1996–2005. The main cause was that the difference in lake levels was narrowing with the supply from CC to DC until the lake levels of both lakes were consistent in 2006. However, as the lake level continued to increase, once the level in each lake increased to a particular threshold, the levels of the two lakes were consistent and maintained the same rates thereafter. The average increased rate of the lake was 0.41 m/y from 2006 to 2014, and the increased rate during 2011–2014 (0.53 m/y) was faster than that during 2006–2011 (0.34 m/y).

4.3. Lake water storage change

As shown in Fig. 4b, the lake area of CC decreased by 0.5 km^2 from 2003 to 2004, and the lake level and water storage decreased by 0.3 m and 0.14 km^3, respectively, during this period. The lake area of DC

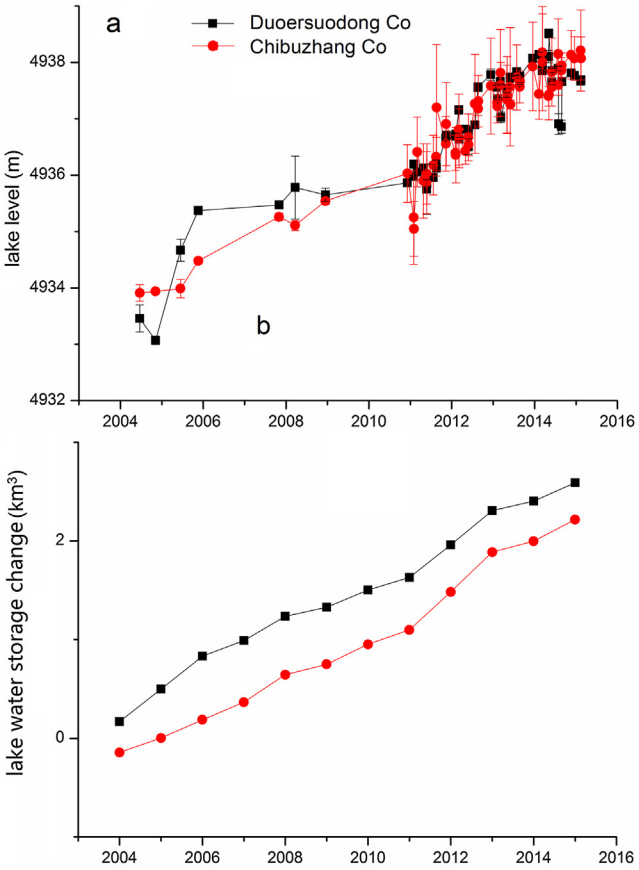

Fig. 4. Lake level and water storage changes from 2003 to 2014. a, lake level; b, water storage change.

increased by 9.5 km^2, and the lake level and water storage increased by 0.38 m and 0.17 km^3, respectively, from 2003 to 2004. The lake water storage began to increase after 2004, and the increased rate of DC (0.22 km^3/y) was higher than that of CC (0.18 km^3/y) from 2003 to 2014. The increased water storage of DC and CC was 2.4 km^3 and 2 km^3, respectively, over the period 2003–2014. The greatest increase in water storage of CC was 0.38 km^3 during 2011–2012 and 0.4 km^3 during 2012–2013, and the increase was 0.33 km^3 and 0.35 km^3 in DC during the same periods, respectively. Water storage in DC and CC had increased by 24.5% and 14.1% since 2003, respectively.

4.4. Inter-annual variations in meteorological factors

As shown in Fig. 5, we analyzed only the change trends in the annual precipitation, annual average temperature and annual evaporation from 1976 to 2013. The average precipitation was 309.5 mm/y, ranging from 190.9 mm (1994) to 529.9 mm (2005) during 1979–2013. It also showed a significant variation, with an average of 281.8 mm/y, ranging from 190.9 mm (1994) to 413.2 mm (1996) during 1979–2000, followed by a slight increased trend with significant variation. The average annual precipitation was 356.4 mm/y, ranging from 221.8 (2006) to 529.9 mm (2005) during 2001–2013 (Fig. 5a). The linear regression method with SPSS software was used to calculate the rates of increase or decrease. The annual average temperature exhibited a significantly increased trend with a rate of 0.026 °C/y (R^2 = 0.39; P less than 0.05), and the annual average temperature was −5.76 °C during 1979–2013 (R^2 = 0.67). The lowest annual average temperature occurred in 1997, with an annual average temperature of −7.8 °C (Fig. 5b). The annual evaporation showed significant variation, with an increased trend (2.5 mm/y, R^2 = 0.67, P less than 0.01), ranging from 1194.1 mm (1979) to 1354.1 mm (1999) during 1976–2013, and the

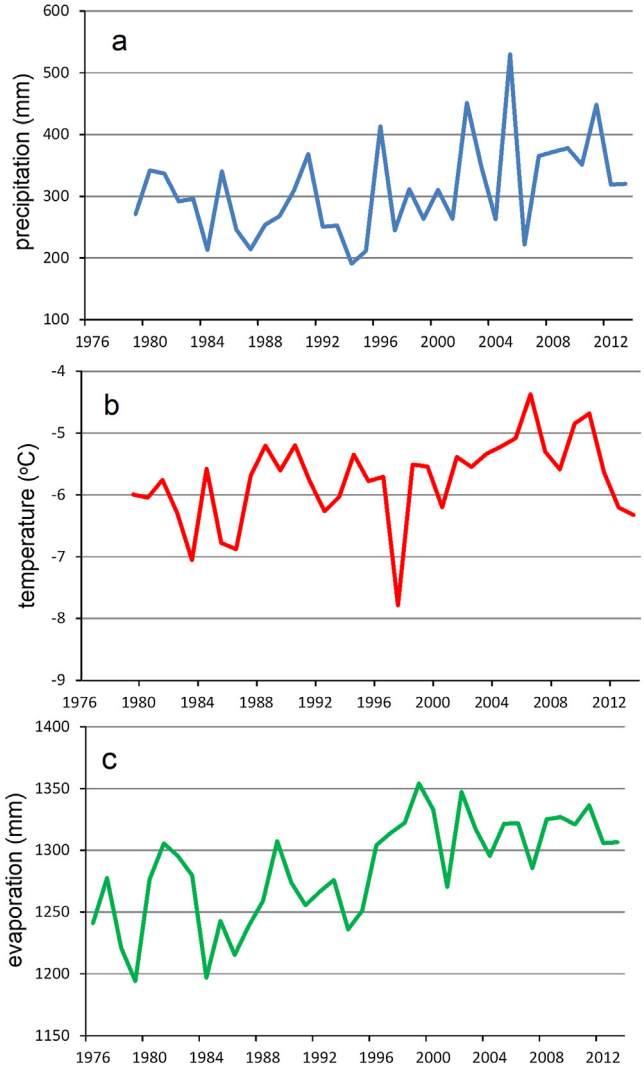

Fig. 5. Changes in meteorological factors from 1976 to 2013. a, precipitation; b, temperature; c, evaporation.

average evaporation was 1284.7 mm/y during this period (Fig. 5c).

The change trends in the monthly precipitation and average monthly temperature are shown in Fig. 6. The lowest temperatures mainly occurred in November, December, January and February. The highest temperatures mainly occurred in June, July and August, and the average temperature in August was approximately 5 °C, with a significantly increased trend from 1979 to 2013 (Fig. 6a). Most of the precipitation mainly occurred in June, July, August, and September, with significant variations (Fig. 6b). The precipitation showed a decreasing trend from 1979 to 1985 and then increased with significant variations until 2013. The precipitation levels in 2005 and 2007 were lower than those in other years.

5. Discussion

5.1. Uncertainties in water storage estimation based on bathymetric data

Using bathymetric and altimetry data is an effective method to estimate lake water storage change (Qiao et al., 2017; Song et al., 2013; Zhang et al., 2017). However, there are certain uncertainties in lake water storage estimation based on underwater topography because bathymetric data only cover part of the lake. Estimating lake water storage change using an empirical equation based on altimetry data and Landsat images provides much higher precision than that achieved with

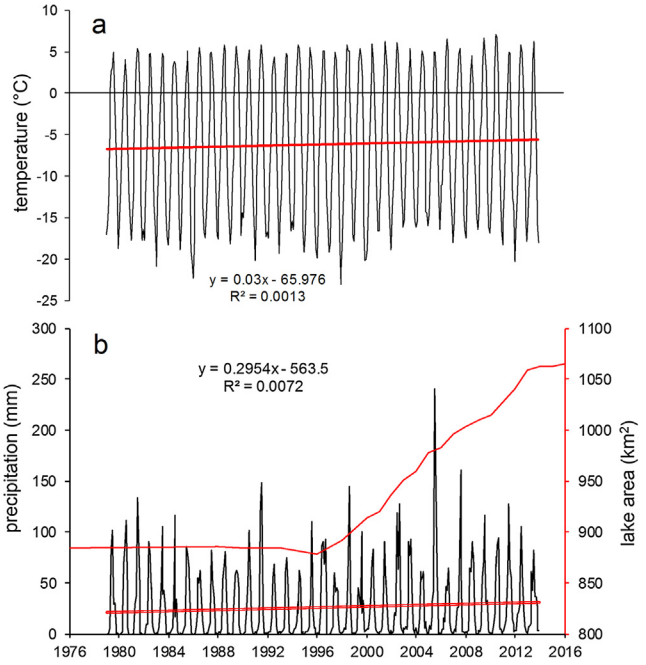

Fig. 6. The change trend of the average monthly temperature (a), monthly precipitation (black line and x-axis) and lake area during the period 1976–2016 (red line and x-axis) (b). (For interpretation of the references to color in this figure legend, the reader is referred to the web version of this article.)

bathymetric data. We considered the results of water storage change from altimetry data as a "truth value" to compare the accuracy of bathymetric data.

Bathymetric data of Bangdag Co from Qiao et al. (2017) covered the main area of the lake, which could be used to estimate changes in water storage by combining Landsat images. We also estimated the water storage change in Bangdag Co based on altimetry data (ICESat and Cryosat-2) and Landsat images from 2004 to 2014, except for 2006, 2009 and 2013 (missing data), and compared the accuracy of the two results. The error was much larger when water storage underwent a small change (e.g., 2004–2005 and 2010–2011), and the error was lower when water storage underwent a large change (e.g., 2004–2008 and 2011–2014). The error in the estimated change in lake water storage based on bathymetric data was 12.8% with respect to the results from altimetry data; therefore, we considered that the error of lake water storage estimation was approximately 12.8%.

Lake water storage change can also be estimated by combining the underwater topography from bathymetric data and data on changes in lake water level, and comparing these results with the results from altimetry data and Landsat images. The assumption is that the lake level from 2014 to 2016 was consistent because the lake area changed little during this period. The results from altimetry data suggested a larger change compared with the results derived from bathymetric data (Table 2), with an error of 23.2%, which was larger than the error for the results of Bangdag Co (12.8%). The reason for this difference could be that bathymetric data were not available for part of the area with increased water storage, e.g., the western part of DC and the southeastern part of CC.

5.2. Geological conditions

Because the terrain of the TP is complex, the topography around the lakes has an important influence on lake changes. Upstream lakes receive glacial meltwater directly from glaciers that supply downstream lakes, and the area and level of upstream lakes remain stable, whereas downstream lakes continue to expand quickly (Qiao and Zhu, 2017; Song and Sheng, 2016). Water seepage may be an important cause of

Table 2
Comparison of the accuracy of water storage change estimation between bathymetric and altimetry data.

Lake	Period	Bathymetric (km^3)[a]	Altimetry (km^3)[b]	Error (km^3)	Percentage (%)[c]
Bangdag Co	2004–2005	0.016	0.041	0.025	0.616
	2005–2007	0.207	0.174	−0.033	−0.189
	2007–2008	0.181	0.217	0.036	0.165
	2004–2007	0.223	0.215	−0.007	−0.034
	2004–2008	0.404	0.431	0.027	0.063
	2005–2008	0.388	0.390	0.001	0.003
	2010–2011	0.026	0.078	0.052	0.665
	2010–2012	0.140	0.184	0.043	0.235
	2010–2014	0.306	0.376	0.070	0.187
	2011–2012	0.114	0.105	−0.009	−0.090
	2011–2014	0.279	0.295	0.016	0.054
	2012–2014	0.165	0.190	0.024	0.129
DC and CC	2006–2007	0.255	0.335	0.080	0.239
	2007–2008	0.654	0.859	0.205	0.238
	2008–2009	0.805	1.056	0.251	0.238
	2009–2010	1.095	1.434	0.339	0.236
	2010–2011	1.304	1.706	0.402	0.236
	2011–2012	1.857	2.422	0.565	0.233
	2012–2013	2.449	3.174	0.725	0.229
	2013–2014	2.615	3.380	0.765	0.226

Note: [a] water storage change from bathymetric data; [b] water storage change from altimetry data; [c] the results of Percentage by Error in the estimate of the volume / Estimate of the volume done by altimetry data.

lake change, and Nam Co may have been affected by seepage, because of a lake water imbalance based on the observed water surface evaporation and river runoff data (Zhou et al., 2013). Phan et al. (2013) analyzed the relationship between TP lakes and glacial runoff based on geometric characteristics, indicated that TP lakes depend more or less on glacial meltwater in which there were glaciers in these watersheds.

As shown in Fig. 7, the two lakes were connected in 1973; however, the channel was narrow, and the lake water supply from the CC was limited because a dam intercepted the water from the CC. It was difficult for the two lakes to reach the same level in a short time, and both lakes remained stable during 1988–1993. However, the lake area of DC began to increase quickly after 1993, and the channel connecting the dam began to widen with the rising lake level. However, CC remained in a stable state, suggesting that most of the increased water storage in CC was supplied to DC. The lake level of the two lakes was consistent in 2006, and the water channel was sufficiently wide for water to flow from CC to DC until the lake levels equalized, suggesting that the geological conditions around the lake are an important factor

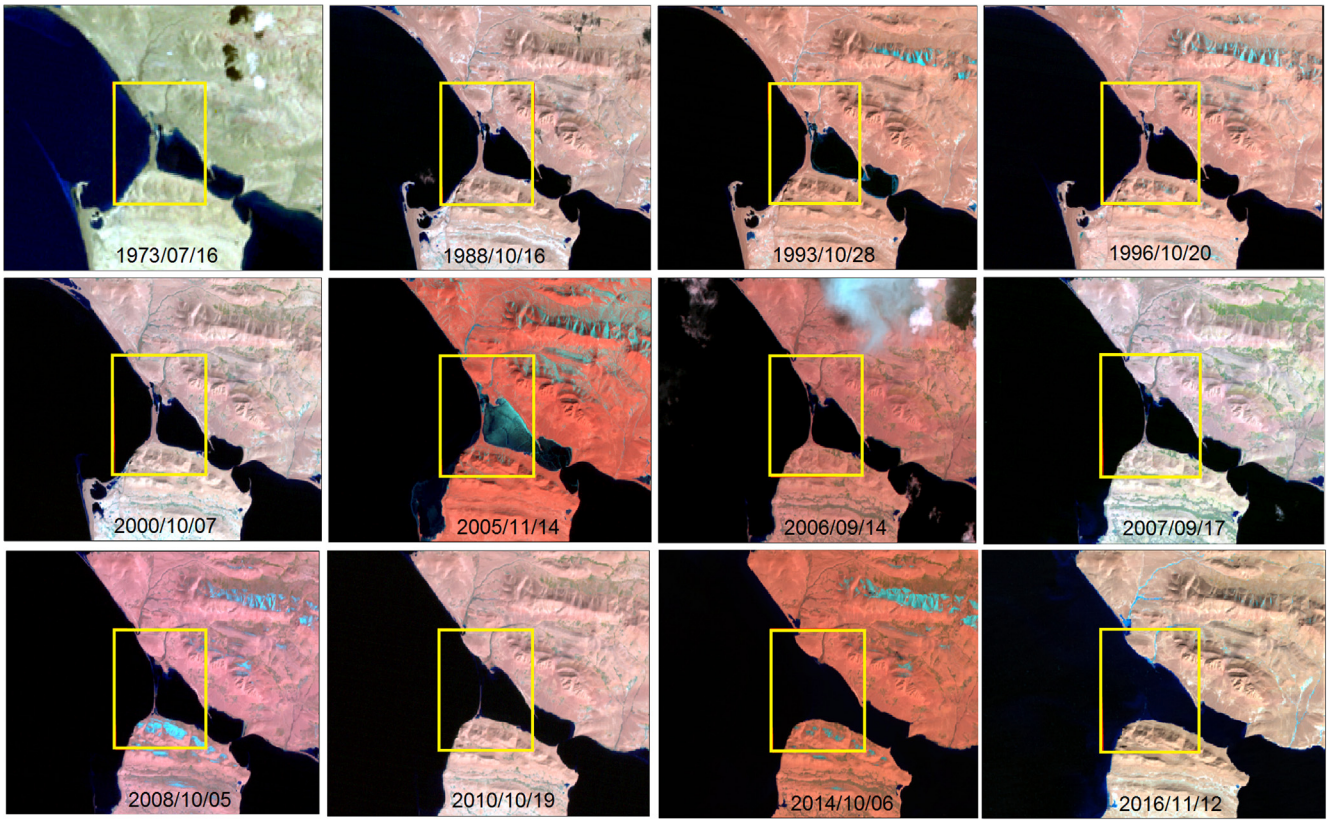

Fig. 7. Topography change in the channel between Chibuzhang Co and Duoersuodong Co from 1973 to 2016.

in lake changes.

5.3. Climate factors

Changes in precipitation and evaporation have direct impacts on lake changes, and glacial meltwater increases with rising temperatures. As shown in Fig. 6b, even though the precipitation had a fluctuating increased trend, the lake area maintained a steady rate of expansion after 1996, suggesting that the precipitation was not the only cause of lake expansion. The rate of rising temperature was faster during 2000–2006 than that during any other periods, and the average temperature in summer also rose during 1979–2013, which may have increased the flow of glacial meltwater to the lakes. The Geladandong and Puruogangri glaciers have experienced significant shrinkage in recent years (Guo et al., 2015; Liu et al., 2016; Neckel et al., 2014; Wei et al., 2014). Increased evaporation (2.5 mm/y) had little impact on the rising lake level (0.41 m/y) during 2006–2015. Both increased glacial meltwater and precipitation had been considered the main causes of lake expansion. However, due to the lack of observational data and other reliable satellite data, it was difficult to quantify the contribution of the different factors to lake expansion and analyze the main cause of lake changes.

5.4. Glacial meltwater

Most glaciers on the TP have experienced significant retreat in recent years (Yao et al., 2012), and increased glacial meltwater can bring much more glacial water to the lakes. However, the contribution of glacial meltwater to lake expansion is difficult to quantify due to a lack of measurement data and reliable satellite data. Altimetry data (e.g., ICESat or CryoSat-2) were used to calculate glacier surface elevation change (Ke et al., 2015; Neckel et al., 2014), but the altimetry data only covered part of the glacier surface on the TP, which may not represent change in the glacier surface elevation of the glaciers. Multi-temporal DEMs have been widely used to research changes in glacier surface elevation by comparing the differences over times, and these measurements can cover the entire glacier surface (Brun et al., 2017; Li and Lin, 2017; Liu et al., 2016; Zhou et al., 2018). For example, the TerraSAR (TSX) add-on for the Digital Elevation Measurement (TanDEM-X) mission was launched in 2010 by the German Aerospace Center, and the primary objective of this mission was to generate a global, high-accuracy and homogeneous DEM following the high standard of accuracy for high resolution terrain information. TanDEM-X has been widely used to calculate glacier elevation change with high accuracy (Li and Lin, 2017; Liu et al., 2016), and the multi-temporal ASTER is also used to generate new DEMs and calculate glacier surface elevation changes by comparing the difference in DEMs (Brun et al., 2017; Rivera et al., 2005).

Table 3 lists the result of glacier mass balances for the Puruogangri and Geladandong region from different studies which vary in spatial and temporal coverage as well as used techniques. A comparison of these studies indicates a periodic shift in glacier thinning rates over the Puruogangri: balanced or slightly negative glacier mass balance (-0.044 ± 0.015 m w.e.a^{-1}) for the period of 2000–2012 (Huintjes et al., 2015; Neckel et al., 2013) and more negative mass balances (-0.269 ± 0.025 m w.e.a^{-1}) for the period of 2012–2016 (Liu et al., 2016). The mean mass balance for the two periods was consistent with that in the study by Zhang et al. (2018), which was -0.046 ± 0.082 m w.e.a^{-1} and -0.294 ± 0.134 m w.e.a^{-1}, respectively. We thus used the result of 2000–2016 (-0.113 ± 0.068 m w.e.a^{-1}) from Zhang et al. (2018) for the mean glacier mass balance over the Puruogangri. Similar to the case for Puruogangri, the results of the study by Zhang et al. (2018) for the two periods in Geladandong glaciers were also consistent with previous results (Chao et al., 2017; Liu, 2016; Liu et al., 2017). For example, the glacier mass balance of Geladandong was -0.128 ± 0.049 m w.e.a^{-1} during 2000–2012 based on the study by Liu. (2016) and -0.134 ± 0.056 m w.e.a^{-1} during 2003–2009 based on the study by Chao et al. (2017), which was consistent with the results of in Zhang et al. (2018), namely, -0.143 ± 0.008 m w.e.a^{-1}. Furthermore, the lacier mass balance for the eastern part of the Geladandong glaciers was -0.155 ± 0.048 m w.e.a^{-1} during 2000–2012 based on the study by Liu. (2016), which was also consistent with the result in the study by Zhang et al. (2018), namely, -0.146 ± 0.008 m w.e.a^{-1}. We thus used the 2000–2016 result (-0.243 ± 0.066 m w.e.a^{-1}) from Zhang et al. (2018) for the mean glacier mass balance over the Geladandong. Glaciers in our study region are located in the western Puruogangri and eastern Geladandong, and the glacier areas were 91.55 km^2 and 74.59 km^2 in 2007, respectively, according to the second Chinese glacier inventory (Guo et al., 2015), which constituted 21.8% and 32.5% of the glaciers area found by Zhang et al. (2018), respectively.

We used the mean glacier mass balance results from Zhang et al. (2018) to estimate glacial meltwater in this study. The two lakes receive glacial meltwater from the eastern glaciers of Puruogangri and western glaciers of Geladandong, and the amount of glacial meltwater from the two glaciers was approximately 0.01 ± 0.006 km^3/y and 0.067 ± 0.018 km^3/y from 2000 to 2016, respectively, based on glacier area and mass balance data. The assumption was that all glacial meltwater supplied to the two lakes was through runoff with minimal evaporation, which contributed approximately 19.3 ± 4.5% of the total lake expansion of DC and CC (0.4 km^3/y) from 2003 to 2014.

6. Conclusion

In this study, we used bathymetric data to acquire underwater topography data using a spatial interpolation method for two lakes (DC and CC) on the central TP. The maximum depth and water storage of the two lakes were 68.7 m and 12.2 ± 1.72 km^3, respectively, with an area of 490.2 km^2 for DC and 116.3 m and 16.2 ± 2.27 km^3, respectively, with an area of 575.4 km^2 for CC in 2016. The increased water storage in DC and CC was 2.4 km^3 and 2 km^3, respectively, from 2003 to 2014 based on satellite altimetry data (ICESat and Cryosat-2) and Landsat images. The relationship between lake change and meteorological factors, indicated that increased glacial meltwater and increased precipitation were important causes for lake expansion, whereas increased evaporation (2.5 mm/y) had little impact on lake expansion (0.41 m/y). The heterogeneous change in the two lakes from 1993 to 2005 was mainly due to water from CC being supplied to DC through a channel, and the lake level of DC was always lower than that of CC until 2006, indicating that the geological condition around a lake is also an important factor in lake change. The glacial meltwater from the Puruogangri and Geladandong glaciers, which supplied water to DC and CC, was approximately 0.01 ± 0.006 km^3/y and 0.067 ± 0.018 km^3/y, respectively, during 2000–2016 based on MODIS albedo products (Zhang et al., 2018). Under the assumption that all glacial meltwater was supplied to the two lakes through runoff with minimal evaporation, glacial meltwater contributed approximately 19.3 ± 4.5% of the total lake expansion of DC and CC (0.4 km^3/y) from 2003 to 2014.

Declaration of Competing Interest

The authors declare that they have no known competing financial interests or personal relationships that could have appeared to influence the work reported in this paper.

Acknowledgments

We thank the editor, associate editor and anonymous reviewers whose suggestions and comments were very helpful in improving this manuscript. This work was supported by the NSFC project (41831177), CAS Strategic Priority Research Program (XDA19020303, XDA20020100), the Ministry of Science and Technology of China

Table 3
Comparison of glacier mass balance estimation for the two regions from published studies.

Glaciers	Mass balance/ m w.e.a^{-1}	Period	Area/km^2	Sources	Method[a]
Puruogangri	−0.044	2001–2011	420	Huintjes et al. (2015)	Phys.
	−0.044 ± 0.015	2000–2012	408	Neckel et al. (2013)	Geod.
	−0.046 ± 0.082	2000–2011	420	Zhang et al. (2018)	Albe.
	−0.269 ± 0.025	2012–2016	420	Liu et al. (2016)	Geod.
	−0.294 ± 0.134	2012–2015	420	Zhang et al. (2018)	Albe.
	−0.113 ± 0.68	2000–2016	420	Zhang et al. (2018)	Albe.
Geladandong	−0.33 ± 0.38	1999–2015	178 (West)[b]	Chen et al. (2017)	Geod.
	−0.134 ± 0.056	2003–2009	845	Chao et al. (2017)	Geod.
	−0.14 ± 0.26	2000–2014	277 (West)	Liu et al. (2017)	Geod.
	−0.128 ± 0.049	2000–2012	845	Liu. (2016)	Geod.
	−0.143 ± 0.08	2000–2011	845	Zhang et al. (2018)	Albe.
	−0.089 ± 0.048	2000–2012	185 (West)	Liu. (2016)	Geod.
	−0.202 ± 0.079	2000–2011	185 (West)	Zhang et al. (2018)	Albe.
	−0.155 ± 0.048	2000–2012	660 (East)[c]	Liu. (2016)	Geod.
	−0.146 ± 0.08	2000–2011	660 (East)	Zhang et al. (2018)	Albe.
	−0.243 ± 0.066	2000–2016	845	Zhang et al. (2018)	Albe.

Note: [a] Geod., geodetic method; Glac., glaciological method; Albe., albedo – based method; Phys., physical model – based method (Zhang et al., 2018); [b] glaciers in the western of Geladandong (Zhang et al., 2018); [c] glaciers in the eastern of Geladandong (Zhang et al., 2018).

Project (2018YFB05050000), the Second Tibetan Plateau Scientific Expedition and Research (STEP) (2019QZKK0202), the CAS Alliance of Field Observation Stations (KFJ-SW-YW038), and the Open Research Fund of Key Laboratory of Tibetan Environmental Changes and Land Surface Processes, Chinese Academy of Sciences (TEL201802). We obtained the China Meteorological Forcing Dataset from the Center of Science Data on the Tibetan Plateau (http://www.tpedatabase.cn).

Appendix A. Supplementary data

Supplementary data to this article can be found online at https://doi.org/10.1016/j.jhydrol.2019.124052.

References

Brun, F., Berthier, E., Wagnon, P., Kaab, A., Treichler, D., 2017. A spatially resolved estimate of High Mountain Asia glacier mass balances, 2000–2016. Nat. Geosci. 10, 668–673.
Chao, N.F., Wang, Z.T., Hwang, C., Jin, T.Y., Cheng, Y.S., 2017. Decline of Geladandong Glacier Elevation in Yangtze River's Source Region: Detection by ICESat and Assessment by Hydroclimatic Data. Remote Sens. 9, 75.
Guo, W.Q., Liu, S.Y., Xu, J.L., Wu, L.Z., Shangguan, D.H., Yao, X.J., Wei, J.F., Bao, W.J., Yu, P.C., Liu, Q., Jiang, Z.L., 2015. The second Chinese glacier inventory: data, methods and results. J. Glaciol. 61 (226), 357–372.
He, J., Yang, K., 2011. China Meteorological Forcing Dataset. Cold and Arid Regions Science Data Center at Lanzhou, China.
Huang, L., Wang, J.B., Zhu, L.P., Ju, J.T., Daut, G., 2017. The warming of large lakes on the Tibetan Plateau: evidence from a lake model simulation of Nam Co, China, during 1979–2012. J. Geophys. Res. Atmos. 122 (24), 13095–13107.
Huffman, G.J., Adler, R.F., Bolvin, D.T., Gu, G., Nelkin, E.J., Bowman, K.P., Hong, Y., Stocker, E.F., Wolff, D.B., 2007. The TRMM multi-satellite precipitation analysis (TMPA): quasi-global, multiyear, combined-sensor precipitation estimates at fine scales. J. Hydrometeorol. 8, 38–55.
Huintjes, E., Neckel, N., Hochschild, V., Schneider, C., 2015. Surface energy and mass balance at Purogangri ice cap, central Tibetan Plateau, 2001–2011. J. Glaciol. 61, 1048–1060.
Hutchinson, M.F., 1988. Calculation of hydrologically sound digital elevation models. Sydney, Australia.
Hutchinson, M.F., 1989. A new procedure for gridding elevation and stream line data with automatic removal of spurious pits. J. Hydrol. 106, 211–232.
Immerzeel, W.W., van Beek, L.P., Bierkens, M.F., 2010. Climate change will affect the Asian water towers. Science 328 (5984), 1382–1385.
Jain, M., Andersen, O.B., Dall, J., Stenseng, L., 2015. Sea surface height determination in the Arctic using Cryosat-2 SAR data from primary peak empirical retrackers. Adv. Sp. Res. 55, 40–50.
Jiang, L.G., Nielsen, K., Andersen, O.B., Bauer-Gottwein, P., 2017. Monitoring recent lake level variations on the Tibetan Plateau using CryoSat-2 SARIn mode data. J. Hydrol. 544, 109–124.
Ke, L.H., Ding, X.L., Song, C.Q., 2015. Estimation of mass balance of Dongkemadi glaciers with multiple methods based on multi-mission satellite data. Quatern. Int. 371, 58–66.
Kleinherenbrink, M., Lindenbergh, R.C., Ditmar, P.G., 2015. Monitoring of lake level changes on the Tibetan Plateau and Tian Shan by retracking Cryosat SARIn waveforms. J. Hydrol. 521, 119–131.
Lazhu, Yang K., Wang, J.B., Lei, Y.B., Chen, Y.Y., Zhu, L.P., Ding, B.H., Qin, J., 2015. Quantifying evaporation and its decadal change for Lake Nam Co, central Tibetan Plateau. J. Geophys. Res. Atmos. 121 (13), 7578–7591.
Lee, S., Im, J., Kim, J., Kim, M., Shin, M., Kim, H., Quackenbush, L., 2016. Arctic Sea Ice Thickness Estimation from CryoSat-2 Satellite Data Using Machine Learning-Based Lead Detection. Remote Sens-Basel. 8 (9), 698.
Lei, Y.B., Yao, T.D., Yang, K., Bird, B.W., Tian, L.D., Zhang, X.W., Wang, W.C., Xiang, Y., Dai, Y.F., Lazhu, Zhou, J., Wang, L., 2018. An integrated investigation of lake storage and water level changes in the Paiku Co basin, central Himalayas. J. Hydrol. 562, 599–608.
Lei, Y.B., Yao, T.D., Yi, C.L., Wang, W.C., Sheng, Y.W., Li, J.L., Joswiak, D., 2012. Glacier mass loss induced the rapid growth of Linggo Co on the central Tibetan Plateau. J. Glaciol. 58, 177–184.
Lei, Y.B., Yang, K., Wang, B., Sheng, Y.W., Bird, B.W., Zhang, G.Q., Tian, L.D., 2014. Response of inland lake dynamics over the Tibetan Plateau to climate change. Climatic Change 125 (2), 281–290.
Lei, Y.B., Yao, T.D., Bird, B.W., Yang, K., Zhai, J.Q., Sheng, Y.W., 2013. Coherent lake growth on the central Tibetan Plateau since the 1970s: characterization and attribution. J. Hydrol. 483, 61–67.
Li, G., Lin, H., 2017. Recent decadal glacier mass balances over the Western Nyainqentanglha Mountains and the increase in their melting contribution to Nam Co Lake measured by differential bistatic SAR interferometry. Global Planet. Change 49, 177–190.
Li, L., Li, J., Yao, X.J., Luo, J., Huang, Y.S., Feng, Y.Y., 2014a. Changes of the three holy lakes in recent years and quantitative analysis of the influencing factors. Quatern. Int. 349, 339–345.
Li, Y.K., Liao, J.J., Guo, H.D., Liu, Z.W., Shen, G.Z., 2014b. Patterns and potential drivers of dramatic changes in Tibetan lakes, 1972–2010. Plos one 9 (11), e111890.
Liu, G., Fan, J., Zhao, F., Mao, K., Dou, C., 2017. Monitoring elevation change of glaciers on Geladandong Mountain using TanDEM-X SAR interferometry. J. Mt. Sci. 14, 859–869.
Liu, L., 2016. Glacier Mass Balances in the Tibetan Plateau Observed from SAR Interferometry. University of Chinese Academy of Sciences, Beijing, China.
Liu, L., Jiang, L.M., Sun, Y.D., Yi, C.L., Wang, H.S., Hsu, H., 2016. Glacier elevation changes (2012–2016) of the Puruogangri Ice Field on the Tibetan Plateau derived from bi-temporal TanDEM-X InSAR data. Int. J. Remote Sens. 37, 5687–5707.
Ma, N., Szilagyi, J., Niu, G.Y., Zhang, Y.S., Zhang, T., Wang, B.B., Wu, Y.H., 2016. Evaporation variability of Nam Co Lake in the Tibetan Plateau and its role in recent rapid lake expansion. J. Hydrol. 537, 27–35.
McFeeters, S., 1996. The use of the Normalized Difference Water Index (NDWI) in the delineation of open water features. Int. J. Remote Sens. 17, 1425–1432.
McMahon, T.A., Peel, M.C., Lowe, L., Srikanthan, R., McVicar, T.R., 2013. Estimating actual, potential, reference crop and pan evaporation using standard meteorological data: a pragmatic synthesis. Hydrol. Earth Syst. Sc. 17 (4), 1331–1363.
Meng, K., Shi, X.H., Wang, E.Q., Liu, F., 2011. High-altitude salt lake elevation changes and glacial ablation in Central Tibet, 2000–2010. Chin. Sci. Bull. 57 (5), 525–534.
Neckel, N., Braun, A., Kropáček, J., Hochschild, V., 2013. Recent mass balance of the Purogangri Ice Cap, central Tibetan Plateau, by means of differential X-band SAR interferometry. The Cryosphere 7, 1623–1633.
Neckel, N., Kropácek, J., Bolch, T., Hochschild, V., 2014. Glacier mass changes on the Tibetan Plateau 2003–2009 derived from ICESat laser altimetry measurements. Environ. Res. Lett. 9, 014009.
Nielsen, K., Stenseng, L., Andersen, O.B., Villadsen, H., Knudsen, P., 2015. Validation of CryoSat-2 SAR mode based lake levels. Remote Sens. Environ. 171, 162–170.
Penman, H.L., 1948. Natural evaporation from open water, hare soil and grass. Proc. R. Soc. Lond. 193 (1032), 120.
Phan, V.H., Lindenbergh, R., Menenti, M., 2012. ICESat derived elevation changes of Tibetan lakes between 2003 and 2009. Int. J. Appl. Earth Obs. 17, 12–22.
Phan, V.H., Lindenbergh, R.C., Menenti, M., 2013. Geometric dependency of Tibetan

lakes on glacial runoff. Hydrol. Earth Syst. Sc. 17 (10), 4061–4077.
Qiao, B.J., Zhu, L.P., 2017. Differences and cause analysis of changes in lakes of different supply types in the north-western Tibetan Plateau. Hydrol. Process. 31, 2752–2763.
Qiao, B.J., Zhu, L.P., 2019. Difference and cause analysis of water storage changes for glacier-fed and non-glacier-fed lakes on the Tibetan Plateau. Sci. Total Environ. 693, 13399.
Qiao, B.J., Zhu, L.P., Wang, J.B., Ju, J.T., Ma, Q.F., Liu, C., 2017. Estimation of lakes water storage and their changes on the northwestern Tibetan Plateau based on bathymetric and Landsat data and driving force analyses. Quatern. Int. 454, 56–67.
Qiao, B.J., Zhu, L.P., Yang, R.M., 2019. Temporal-spatial differences in lake water storage changes and their links to climate change throughout the Tibetan Plateau. Remote Sens. Environ. 222, 232–243.
Rivera, A., Casassa, G., Bamber, J., Kaab, A., 2005. Ice-elevation changes of Glacier Chico, southern Patagonia using Aster DEMs, aerial photographs and GPS data. J. Glaciol. 51 (172), 105–112.
Sheffield, J., Goteti, G., Wood, E.F., 2006. Development of a 50-year high-resolution global dataset of meteorological forcings for land surface modeling. J. Climate 19 (3), 3088–3111.
Samuelsson, P., Tjernström, M., 2001. Mesoscale flow modification induced by land-lake surface temperature and roughness differences. J. Geophys. Res. 106D, 12419–12435.
Song, C.Q., Huang, B., Ke, L.H., 2013. Modeling and analysis of lake water storage changes on the Tibetan Plateau using multi-mission satellite data. Remote Sens. Environ. 135, 25–35.
Song, C.Q., Huang, B., Ke, L.H., Richards, K.S., 2014a. Seasonal and abrupt changes in the water level of closed lakes on the Tibetan Plateau and implications for climate impacts. J. Hydrol. 514, 131–144.
Song, C.Q., Huang, B., Richards, K., Ke, L.H., Phan, V.H., 2014b. Accelerated lake expansion on the Tibetan Plateau in the 2000s: induced by glacial melting or other processes? Water Resour. Res. 50 (4), 3170–3186.
Song, C.Q., Sheng, Y.W., 2016. Contrasting evolution patterns between glacier-fed and non-glacier-fed lakes in the Tanggula Mountains and climate cause analysis. Climatic Change 135 (3), 493–507.
Song, C.Q., Ye, Q.H., Sheng, Y.W., Gong, T.L., 2015a. Combined ICESat and CryoSat-2 Altimetry for Accessing Water Level Dynamics of Tibetan Lakes over 2003–2014. Water 7 (9), 4685–4700.
Song, C.Q., Ye, Q.H., Cheng, X., 2015b. Shifts in water level variation of Namco in the central Tibetan Plateau from ICESat and CryoSat-2 altimetry and station observation. Chin. Sci. Bull. 60 (14), 1–11.
Thompson, L.G., Tandong, Y., Davis, M.E., Mosley-Thompson, E., Mashiotta, T.A., Lin, P.-N., Mikhalenko, V.N., Zagorodnov, V.S., 2006. Holocene climate variability archived in the Puruogangri ice cap on the central Tibetan Plateau. Ann. Glaciol. 43, 61–69.
Tseng, K.H., Chang, C.P., Shum, C., Kuo, C.Y., Liu, K.T., Shang, K., Jia, Y., Sun, J., 2016. Quantifying Freshwater Mass Balance in the Central Tibetan Plateau by Integrating Satellite Remote Sensing, Altimetry, and Gravimetry. Remote Sens-Basel. 8, 441.
Villadsen, H., Deng, X., Andersen, O.B., Stenseng, L., Nielsen, K., Knudsen, P., 2016. Improved inland water levels from SAR altimetry using novel empirical and physical retrackers. J. Hydrol. 537, 234–247.
Wan, W., Xiao, P.F., Feng, X.Z., Li, H., Ma, R.H., Duan, H.T., Zhao, L.M., 2014. Monitoring lake changes of Qinghai-Tibetan Plateau over the past 30 years using satellite remote sensing data. Chin. Sci. Bull. 59 (10), 1021–1035.
Wang, X.W., Gong, P., Zhao, Y.Y., Xu, Y., Cheng, X., Niu, Z.G., Luo, Z.C., Huang, H.B., Sun, F.D., Li, X.W., 2013. Water-level changes in China's large lakes determined from ICESat/GLAS data. Remote Sens. Environ. 132, 131–144.
Wang, Y., Wang, J.B., Zhu, L.P., Lin, X., Hu, J.F., Ma, Q.F., Ju, J.T., Peng, P., Yang, R.M., 2017. Mid- to late-Holocene paleoenvironmental changes inferred from organic geochemical proxies in Lake Tangra Yumco, Central Tibetan Plateau. Holocene 21 (10), 1475–1486.
Wei, J.F., Liu, S.Y., Guo, W.Q., Yao, X.J., Xu, J.L., Bao, W.J., Jiang, Z.L., 2014. Surface-area changes of glaciers in the Tibetan Plateau interior area since the 1970s using recent Landsat images and historical maps. Ann. Glaciol. 55, 213–222.
Xu, T., Zhu, L.P., Lu, X.M., Ma, Q.F., Wang, J.B., Ju, J.T., Huang, L., 2019. Mid- to late-Holocene paleoenvironmental changes and glacier fluctuations reconstructed from the sediments of proglacial lake Buruo Co, northern Tibetan Plateau. Palaeogeogr. Palaeocl. 517, 74–85.
Xu, Z.X., Gong, T.L., Li, J.Y., 2008. Decadal trend of climate in the Tibetan Plateau-regional temperature and precipitation. Hydrol. Process. 22 (16), 3056–3065.
Yang, R.M., Zhu, L.P., Wang, J.B., Ju, J.T., Ma, Q.F., Turner, F., Guo, Y., 2017. Spatiotemporal variations in volume of closed lakes on the Tibetan Plateau and their climatic responses from 1976 to 2013. Climatic Change 140, 621–633.
Yao, X.J., Li, L., Zhao, J., Sun, M.P., Li, J., Gong, P., An, L.N., 2015. Spatial-temporal variations of lake ice in the Hoh Xil region from 2000 to 2011. Acta Geographica Sinica 70 (7), 1114–1124.
Yao, T.D., Thompson, L., Yang, W., Yu, W.S., Gao, Y., Guo, X.J., Yang, X.X., Duan, K.Q., Zhao, H.B., Xu, B.Q., Pu, J.C., Lu, A.X., Xiang, Y., Kattel, D.B., Joswiak, D., 2012. Different glacier status with atmospheric circulations in Tibetan Plateau and surroundings. Nat. Clim. Change 2 (9), 663–667.
Yi, C.L., Li, X.Z., Qu, J.J., 2002. Quaternary glaciation of Puruogangri - the largest modern ice field in Tibet. Quatern. Int. 97–98, 111–121.
Zhang, B., Wu, Y.H., Zhu, L.P., Wang, J.B., Li, J.S., Chen, D.M., 2011a. Estimation and trend detection of water storage at Nam Co Lake, central Tibetan Plateau. J. Hydrol. 405 (1–2), 161–170.
Zhang, G.Q., Xie, H.J., Kang, S.C., Yi, D.H., Ackley, S.F., 2011b. Monitoring lake level changes on the Tibetan Plateau using ICESat altimetry data (2003–2009). Remote Sens. Environ. 115 (7), 1733–1742.
Zhang, G.Q., Xie, H.J., Yao, T.D., Kang, S.C., 2013. Water balance estimates of ten greatest lakes in China using ICESat and Landsat data. Chin. Sci. Bull. 58 (31), 3815–3829.
Zhang, G.Q., Yao, T.D., Xie, H.J., Zhang, K.X., Zhu, F.J., 2014a. Lakes' state and abundance across the Tibetan Plateau. Chin. Sci. Bull. 59, 3010–3021.
Zhang, G.Q., Yao, T.D., Xie, H.J., Qin, J., Ye, Y.Q.H., Dai, Y.F., Guo, R.F., 2014b. Estimating surface temperature changes of lakes in the Tibetan Plateau using MODIS LST data. J. Geophys. Res. Atmos. 119 (14), 8552–8567.
Zhang, G.Q., Yao, T.D., Xie, H.J., Wang, W.C., Yang, W., 2015. An inventory of glacial lakes in the Third Pole region and their changes in response to global warming. Global Planet. Change 131, 148–157.
Zhang, G.Q., Yao, T.D., Shum, C.K., Yi, S., Yang, K., Xie, H.J., Feng, W., Bolch, T., Wang, L., Behrangi, A., Zhang, H.B., Wang, W.C., Xiang, Y., Yu, J.Y., 2017. Lake volume and groundwater storage variations in Tibetan Plateau's endorheic basin. Geophys. Res. Lett. 44, 5550–5560.
Zhang, Z.M., Jiang, L.M., Liu, L., Sun, Y.F., Wang, H.S., 2018. Annual glacier-wide mass balance (2000–2016) of the interior Tibetan Plateau reconstructed from MODIS albedo products. Remote Sens. 10, 1031.
Zhao, L., Jin, J., Wang, S., Ek, M.B., 2012. Integration of remote-sensing data with WRF to improve lake effect precipitation simulations over the Great Lakes region. J. Geophys. Res. 117, D09102.
Zhou, J., Wang, L., Zhang, Y.S., Guo, Y.H., Li, X.P., Liu, W.B., 2015. Exploring the water storage changes in the largest lake (Selin Co) over the Tibetan Plateau during 2003–2012 from a basin-wide hydrological modeling. Water Resour. Res. 51, 8060–8086.
Zhou, S.Q., Kang, S.C., Chen, F., Joswiak, D.R., 2013. Water balance observations reveal significant subsurface water seepage from Lake Nam Co, south-central Tibetan Plateau. J. Hydrol. 491, 89–99.
Zhou, W.M., Li, Z.W., Li, J., Cui, Z.Y., Wang, C.C., 2014. Variations of glaciers and glacial lake in Geladandong mountain range in 1992–2009 with remote-sensing technology. J. Central South Univ. (Sci. Technol.) 45 (10), 3505–3512.
Zhou, Y.S., Li, Z.W., Li, J., Zhao, R., Ding, X.L., 2018. Glacier mass balance in the Qinghai-Tibet Plateau and its surroundings from the mid-1970s to 2000 based on Hexagon KH-9 and SRTM DEMs. Remote Sens. Environ. 201, 96–112.
Zhou, Y.S., Hu, J., Li, Z.W., Li, J., Zhao, R., Ding, X.L., 2019. Quantifying glacial mass change and its contribution to lake growths in central Kunlun during 2000–2015 from multi-source remote sensing data. J. Hydrol. 570, 38–50.
Zhu, L.P., Xie, M.P., Wu, Y.H., 2010. Quantitative analysis of lake area variations and the influence factors from 1971 to 2004 in the Nam Co basin of the Tibetan Plateau. Chin. Sci. Bull. 55 (13), 1294–1303.